Articles - Discoveries

Molecular and evolutionary mechanisms of yeast thermotolerance

Melanie B. Abrams[1]*, Claire A. Dubin[1]*, Faisal AlZaben[1], Juan Bravo[2], Pierre M. Joubert[1], Carly V. Weiss[1,3], and Rachel B. Brem[1,4]

[1]Department of Plant and Microbial Biology, UC Berkeley, Berkeley, CA; [2]Graduate Program in the Biology of Aging, University of Southern California, Los Angeles, CA; [3]Current address: Department of Biology, Stanford University, Palo Alto, CA; [4]Buck Institute for Research on Aging, Novato, CA

*These authors contributed equally to this work.

Corresponding author: Rachel Brem, rbrem@berkeley.edu

ABSTRACT

Many familiar traits in the natural world—from lions' manes to the longevity of bristlecone pine trees—arose in the distant past, and have long since fixed in their respective species. A key challenge in evolutionary genetics is to figure out how and why species-defining traits have come to be. We used the thermotolerance growth advantage of the yeast *Saccharomyces cerevisiae* over its sister species *Saccharomyces paradoxus* as a model for addressing these questions. Analyzing loci where the *S. cerevisiae* allele promotes thermotolerance, we detected marked sequence divergence from *S. paradoxus*, and conservation within the species, across dozens of *S. cerevisiae* populations. Such patterns are most consistent with a history in which adaptive alleles arose in the ancestor of modern *S. cerevisiae* lineages and have been maintained since then by purifying selection. Since sequence-based signatures of selection were particularly strong at the chromosome segregation gene *ESP1*, we used this locus as a case study for focused mechanistic follow-up. These revealed that, in culture at high temperature, the *S. paradoxus ESP1* allele conferred a striking defect in biomass accumulation and cell division relative to the *S. cerevisiae allele*. Only genetic divergence in the *ESP1* coding region mattered phenotypically, with no functional impact detectable from the promoter. This study of an ancient adaptation, originating via selection at many unlinked loci, sets the precedent for complex evolutionary genetics across deep species divergences throughout Eukarya.

INTRODUCTION

A central goal of research in evolutionary genetics is to understand how new traits are built. Much of the literature to date focuses on adaptive trait innovation within a species, in the wild (Asgari et al., 2020; Chan et al., 2010; Cleves et al., 2014; Field et al., 2016; Linnen et al., 2013; Will et al., 2010) and in the lab (Blount et al., 2012; Castro et al., 2019; Good et al., 2017; Tenaillon et al., 2016). These systems have enabled studies of short-term adaptation, its genetics (Barroso-Batista et al., 2014; Castro et al., 2019; Garud et al., 2015; Good et al., 2017; Harris et al., 2018; Xie et al., 2019) and its dynamics (Blount et al., 2012; Toprak et al., 2011). In several elegant case studies, it has been possible to track parallel adaptations in distinct lineages of a species (Chan et al., 2010; Hoekstra and Nachman, 2003; Rosenblum et al., 2010; Xie et al., 2019).

Such work on recent adaptations serves as a backdrop for the study of evolution over longer timescales. Many familiar traits from the natural world have been acquired over millions of generations. In the modern day, such characters manifest as differences between deeply diverged, reproductively isolated lineages. They can represent the abiding fitness strategies of their respective species, and are thus of particular interest in the field. But their evolutionary mechanisms pose a key challenge, given that the relevant events happened so long ago. For these ancient traits, candidate-gene studies have implicated individual loci (Anderson et al., 2016; Baldwin et al., 2014; Liu et al., 2018; Massey and Wittkopp, 2016; Sackton et al., 2019; Sulak et al., 2016; Tian et al., 2019) and reconstructed the mutational path by which such a gene evolved (Anderson et al., 2015; Bridgham et al., 2009; Finnigan et al., 2012; Liu et al., 2018; Pillai et al., 2020). Even in such landmark cases, the tempo and mode of evolution of deep trait divergences has largely remained out of reach. To meet the latter challenge, one would need to trace the rise of causal alleles in the respective species and the selective forces that drove it, and pinpoint the timing of these events.

In prior work, our group mapped multiple housekeeping genes underlying the difference in thermotolerance between *Saccharomyces cerevisiae* and other species in its clade, and found that *S. cerevisiae* harbored derived alleles at these loci (Weiss et al., 2018). Here we set out to investigate when and how *S. cerevisiae* acquired the putatively adaptive determinants of thermotolerance, using a population-genomic approach. We then used the results as a jumping-off point for additional analyses of the molecular mechanisms by which variants at thermotolerance genes confer their effects.

RESULTS

Pervasive divergence from *S. paradoxus* at *S. cerevisiae* thermotolerance loci

We started by addressing the genetics of *S. cerevisiae* thermotolerance, with the ultimate goal of investigating evolutionary mechanisms of the trait. Our earlier study used genome-scale screens with the reciprocal hemizygosity test (Steinmetz et al., 2002; Stern, 2014) to identify eight genes at which *S. cerevisiae* harbored pro-thermotolerance alleles relative to those of *S. paradoxus* (Weiss et al., 2018). We re-processed these screen data with an improved statistical workflow, to boost power and genome coverage (see Methods). The results recapitulated seven loci that we had reported and validated, plus an additional three that had not risen to

significance in our original analysis (Table S1). We considered the set of ten loci as a more complete model of the genetic architecture of the trait, which would be well-suited to population and evolutionary analyses.

Thermotolerance is a defining and putatively adaptive character of *S. cerevisiae*, shared among isolates within the species (Gonçalves et al., 2011; Salvadó et al., 2011; Sweeney et al., 2004). In our genetic mapping of the trait, we used wild European *S. cerevisiae* (strain DVBPG1373, from the Netherlands, compared against the UK *S. paradoxus* strain Z1). Did the *S. cerevisiae* alleles of the resulting mapped genes arise under positive selection, in the European population or elsewhere? As a first strategy to address this, we made use of a broad population survey of *S. cerevisiae* (Peter et al., 2018), and the deepest-sampled *S. paradoxus* populations available (from vineyards and European collection locales (Bergström et al., 2014) and from North America (Durand et al., 2019)). With these sequences, between the species we computed the absolute diversity statistic D_{xy}, which reaches high levels in a lineage after selection when compared to a representative of the ancestral state (Nei, 1987). We found enrichment for high D_{xy} among our mapped thermotolerance genes, using each population pair of *S. cerevisiae* and *S. paradoxus* in turn (Table S2). Thus, divergence from *S. paradoxus* at thermotolerance loci is a trend that pervades >30 *S. cerevisiae* populations, collected in Europe, Asia, Africa, and the Americas. A model of parallel innovation in each such population is unlikely on the basis of parsimony; rather, if our focal genes evolved under positive selection, the selective event would likely have predated the radiation of modern *S. cerevisiae*.

Thermotolerance loci are conserved within *S. cerevisiae*

We next sought to investigate the more recent history of thermotolerance loci across *S. cerevisiae* lineages. If an ancestral population of this species had acquired thermotolerance alleles under positive selection, these sequence determinants could have been maintained since then under continued negative selection. Alternatively, the pressure could have relaxed in more recently colonized niches. We reasoned that haplotype-level tests would afford better power to explore this than site-by-site calculations, and for this purpose we used the SelectionHapStats suite (Garud et al., 2015; Harris et al., 2018). Haplotype frequencies inferred by this tool can be used to detect very recent soft selective sweeps in young populations or, for a putatively ancient adaptation like ours, to report conservation more generally. We inferred multi-locus genotypes (MLGs, which are analogous to haplotypes for unphased genotype data)

in each of the five *S. cerevisiae* populations for which the most strain data were available. Then, for each population separately, we calculated summary statistics from MLG frequencies in sequence windows of each gene in turn. We first focused on the expected homozygosity G1, the sum of the squares of MLG frequencies, which is elevated around a selected site after a sweep as a product of strong allele-sharing (Garud et al., 2015; Harris et al., 2018). Resampling analyses revealed high values of G1 at thermotolerance genes relative to the genome as a whole, significantly so in three *S. cerevisiae* populations (Table 1 and Table S3A).

Next, we used our SelectionHapStats pipeline to calculate G2, the homozygosity attributable to all MLGs except the most common one, and the ratio G2/G1. As with our analysis of G1, resampling tests on G2/G1 again highlighted thermotolerance genes as unique against the genomic background, but in this case the direction was reversed: G2/G1 values among our gene set were significantly low in several *S. cerevisiae* populations (Table 1 and Table S3B). Together, results from this approach make clear that thermotolerance loci have a particularly high degree of allele-sharing, and uncommon MLGs contribute particularly little to these patterns—implicating the most common MLG as the driver of the allele-sharing signal. In other words, thermotolerance loci exhibit sequence conservation within *S. cerevisiae* populations, a hallmark of purifying selection in the latter.

We anticipated that inspecting allele-sharing at high resolution across genomic loci could further help reveal facets of the history of thermotolerance genes. Using the large vineyard and European population of *S. cerevisiae*, we found that G1 was not uniform across a given thermotolerance gene, and for most loci, peaks of allele-sharing could be resolved (Figure 1A and Figure S1). As expected, such peaks corresponded to troughs of polymorphism across the population, measured by the number of pairwise differences between strains (π); likewise, low allele-sharing correlated with high polymorphism (Figure S1).

Notably, even at peaks of allele-sharing in thermotolerance loci in wine/European *S. cerevisiae*, in absolute terms genotype homozygosity was modest. In the top-scoring regions in the wine/European population (at the 5' end of the chromosome segregation gene *ESP1;* Figure 1A), G1 reached at most a value of 0.15. This is consistent with our inference of an ancient date for positive selection at *ESP1* and other loci, since the tight conservation and long haplotypes expected immediately after selection would be eroded over longer timescales (Berry et al., 1991; Smith and Haigh, 1974; Weigand and Leese, 2018). We observed similar spatial patterns

at *ESP1* in the other *S. cerevisiae* populations in which we had detected allele-sharing in general across thermotolerance genes (Figure 1B-C), indicating that all these populations likely have had the same forces at play at the locus.

Molecular evolution and functional impact of coding variation at *ESP1*

The maximal signal of allele-sharing we detected at *ESP1* in *S. cerevisiae* populations (Figure 1, Table S1A) dovetailed with its dramatic phenotypic effect, upon allele replacement between *S. cerevisiae* and *S. paradoxus* (Weiss et al., 2018). Given this evidence for evolutionary and functional importance of variation at *ESP1*, we chose to use it as a test case to achieve deeper molecular insight in the thermotolerance system. We first aimed to contrast the role of coding and *cis*-regulatory divergence between species at *ESP1*. We used the branch-site model of the PAML suite (Yang, 2007) for phylogenetic analyses of the *ESP1* coding sequence in *Saccharomyces sensu stricto* species. The results revealed significant evidence for accelerated protein evolution along the *S. cerevisiae* lineage of *ESP1* ($p = 0.046$), though we could not resolve signal at individual codons (see Methods). Thus, *S. cerevisiae* harbors unique amino acid changes at sites otherwise conserved across sister species.

Such a molecular-evolution signature in the *ESP1* open reading frame suggested that divergence between species in this region would have a particularly strong impact on thermotolerance. We tested this experimentally by introducing the *ESP1* coding region and, separately, the *ESP1* promoter, from wild *S. paradoxus* (strain Z1) into a wild *S. cerevisiae* background (strain DVBPG1373). Growth experiments revealed a dramatic, temperature-dependent effect of variation in the *ESP1* coding region, with the *S. paradoxus* allele compromising growth at under heat treatment (Figure 2 and Figure S2). This transgenic fully recapitulated the impact of a larger, regional swap of the *S. paradoxus* open reading frame and promoter together into *S. cerevisiae* (Figure 2 and Figure S2). By contrast, species divergence in the *ESP1* promoter had no effect on thermotolerance, when analyzed on its own (Figure 2 and Figure S2). As an independent analysis of potential promoter effects, we inspected *cis*-regulatory variation between *S. cerevisiae* and *S. paradoxus* in measurements of *ESP1* gene expression. We detected no striking *cis*-regulatory divergence, at *ESP1* in particular or across thermotolerance genes as a set (Table S4). Likewise, the latter yielded no signal in a test for non-neutral directional *cis*-regulatory change ((Bullard et al., 2010); Table S4). These data highlight the evolutionary and functional importance of amino acid variation between *S.*

cerevisiae and *S. paradoxus* at *ESP1,* and raise the possibility that coding divergence may also prove to underlie the thermotolerance effects of other mapped loci.

Temperature dependence and cell biology of species divergence effects at *ESP1*

In further pursuit of the molecular mechanisms of *S. cerevisiae* thermotolerance, we turned to the potential for clues from temperature-dependent genetics. *S. cerevisiae* outperforms its sister species at a range of elevated temperatures (Salvadó et al., 2011; Sweeney et al., 2004). Our thermotolerance loci were identified in a screen for effects of interspecies divergence at 39°C (Weiss et al., 2018), and their relevance to growth under other conditions is unknown. Using *ESP1* as a case study to address this question, we assayed biomass accumulation of wild-type and *ESP1* transgenic strains under a temperature dose-response. In these growth experiments, we observed a gradual decline in *S. cerevisiae* and *S. paradoxus* growth as temperature increased, with the latter more sensitive to heat as expected (Figure 3). An allele-swap strain in the *S. cerevisiae* background harboring *S. paradoxus ESP1* exhibited a sharp drop in growth at ~38°C; it grew readily below this temperature, phenocopying the wild-type *S. cerevisiae* progenitor, and at higher temperatures, it exhibited the negligible growth seen in wild-type *S. paradoxus* (Figure 3). Such a dose-response, resembling the sigmoidal behavior of a cooperative biochemical process, was a synthetic property of the *ESP1* inter-species swap, distinguishing it from either wild-type species. These data imply that, at least in the *S. cerevisiae* background, the function of *S. paradoxus* Esp1 breaks down with a steep temperature dependence, whose midpoint is close to the conditions under which this gene was originally identified (39°C).

ESP1 encodes separase, which releases sister chromatids for separation into daughter cells during anaphase, cleaving the cohesin ring that has held them together in metaphase. We reasoned that, if *S. paradoxus* Esp1 failed to function, in actively growing cells harboring this allele we would see hallmarks of arrest late in the cell cycle. Quantitative microscopy bore out this prediction: as in wild-type *S. paradoxus* (Weiss et al., 2018), large-budded dyads predominated in cultures of the *S. cerevisiae* transgenic with *S. paradoxus ESP1*, when incubated at 39°C (Figure 4). These findings are consistent with a mechanism in which heat treatment compromises separase function of the *S. paradoxus* allele of Esp1, blocking the progress of the cell cycle and limiting viability and biomass accumulation. Evolution in *S.*

cerevisiae would have resolved these defects, introducing genetic changes that foster Esp1 function and boost fitness at high temperature.

DISCUSSION

In the study of adaptation, a trait that arises in a species, goes to fixation, and is maintained for thousands of generations can be seen as the ultimate evolutionary success story. In this work, we used yeast thermotolerance as a model of this process. We shed light on why and when the trait was acquired in *S. cerevisiae*, and we established key elements of the molecular genetics and cell biology of divergent alleles at the underlying loci.

Our sequence analyses yielded a clear inference of the selective forces driving thermotolerance. Divergence between *S. cerevisiae* and *S. paradoxus* at thermotolerance loci, and conservation within *S. cerevisiae*, strongly suggest an innovation in ancestral *S. cerevisiae* maintained by purifying selection into the modern day. Also consistent with the latter model is the fact that at a given thermotolerance locus, alleles from *S. cerevisiae* isolates from around the world were partially sufficient for the trait, when swapped into a poorly-performing *S. paradoxus* background (Weiss et al., 2018). Plausibly, the initial rise of thermotolerance early in *S. cerevisiae* history could have been driven by the ecology of hot East Asian niches where the species likely originated (Peter et al., 2018).

Such a scenario for thermotolerance sets up an intriguing contrast against traits that undergo independent, parallel adaptations in distinct lineages of a species (Chan et al., 2010; Hoekstra and Nachman, 2003; Rosenblum et al., 2010; Xie et al., 2019). Under one compelling model, thermotolerance alleles acquired by an initially small, specialized *S. cerevisiae* ancestor could have enabled later migrants to colonize other warm niches (Robinson et al., 2016). That said, additional lineage-specific adaptations to heighten thermotolerance further could also eventually come to light.

If we were to achieve a complete picture of the origins of thermotolerance, we would need to pinpoint exactly how adaptive alleles arose and swept through *S. cerevisiae*, putatively before the radiation of modern lineages. For complex traits in sexual species, theory predicts that adaptation will be fastest when beneficial alleles at many loci are segregating in the population, of which an individual needs to acquire only a subset to advance in fitness (Lynch, 2010; Neher

et al., 2010). Thermotolerance in *S. cerevisiae* conforms to the features of the latter theoretical models: it is highly complex, and for most genes we have mapped thus far, *S. cerevisiae* alleles confer growth advantages when tested in isolation (Weiss et al., 2018). *A priori*, then, a scenario of partial selective sweeps may prove to be the best description of thermotolerance evolution in ancestral *S. cerevisiae*.

And what were the mechanisms of these putative ancient sweeps? We have seen that at the average thermotolerance locus, secondary genotypes segregate at particularly low frequencies relative to the most common genotype. This suggests a process of hard selective sweeps in ancestral *S. cerevisiae*—waves of innovation and refinement yielding one major adaptive pro-thermotolerance genotype per locus in the ancestral population, which would come down through modern lineages and predominate in extant strains. However, we cannot rule out a soft selective sweep (Messer and Petrov, 2013) at a given locus in the ancestral population: if many adaptive genotypes were segregating at that point in history, all but one could have been lost by drift alone during the later radiation of *S. cerevisiae*. Indeed, each of these models might be the right answer for some subset of thermotolerance loci. Given the complexity of the trait, we anticipate that evolution will have used multiple mechanisms to build it, across time and throughout populations.

Our data also leave open the question of which divergent sites at a given gene underlie *S. cerevisiae* thermotolerance. A primary role for protein-coding variation, as we have seen for *ESP1*, would echo decades of evo-devo literature on this theme (Hoekstra and Coyne, 2007; Wray, 2007). Furthermore, given how much our temperature dose-response of *ESP1* function looks like a two-state protein unfolding curve, it is tempting to speculate that the *S. cerevisiae* allele of this gene may act by boosting protein stability. If such a mechanism were to prove the general rule for our loci, it would dovetail with the trend for proteome thermostability seen in heat-tolerant species (Leuenberger et al., 2017). Future work will be necessary to test whether *S. cerevisiae* truly has tweaked its protein biophysics to meet the challenges of growth at high temperature, and how this might compare with the evolution of thermotolerance in other systems (Sas-Chen et al., 2020).

In fact, our work has set a precedent by which evolutionary-genetic principles for many other ancient traits may come within reach. The paradigm we have used here combines methods for inter-species genetics (Weiss and Brem, 2019) with population-genomic and molecular-

evolution tools. This setup is generally applicable across Eukarya; and with it, once we know the genes that govern a species-defining trait, we can look far back in history and figure out how it came to be.

METHODS

Identifying thermotolerance genes

To identify genes at which variation between *S. cerevisiae and S. paradoxus* impacts thermotolerance, we re-analyzed data from a reciprocal hemizygosity screen of transposon mutants in the interspecies hybrid background (Weiss et al., 2018) as described, with the following exceptions. Call $a_{39,i}$ the average, across technical replicates, of sequencing-based abundances of a hemizygote mutant measured after 5-6 generations in biological replicate *i* of growth at 39°C, and $a_{28,i}$ the analogous quantity for growth at 28°C. We tabulated three replicate estimates of the temperature effect on growth of the mutant as $\log2(a_{39,i}/a_{28,i})$ for i = (1,3). If the coefficient of variation across these biological replicates was greater than 20.0, we eliminated the mutant from further consideration. Otherwise, for a given gene, we concatenated these vectors of length three across all hemizygote mutants in the *S. paradoxus* allele for which we had abundance data, yielding the set of temperature effects s_{Spar}. We did likewise for the *S. cerevisiae* allele, yielding s_{Scer}. We retained for further analysis only genes at which either of these two vectors was of length two or greater. For each such gene, we compared s_{Scer} and s_{Spar} with a Wilcoxon test, and corrected for multiple testing across genes, as described. Instructions and scripts are available from the authors.

Sequence data, alignments, and interspecies diversity

For D_{XY} analyses in Table S2, for a given gene, open reading frame sequences for the strains of each *S. cerevisiae* population from (Peter et al., 2018) were aligned against the European *S. paradoxus* population from (Bergström et al., 2014) and, separately, against the North American *S. paradoxus* subpopulation B from (Durand et al., 2019). Alignments used MUSCLE (Edgar, 2004) with the default settings for DNA and --maxiters set to 2. Any gene for which, in the alignment, >10% of sites were denoted as gaps or unknown nucleotides (Ns), or sequences from <75% of strains in the population were available, was eliminated from analysis, leaving 4110 to 4781 genes suitable for testing in each population.

We calculated pairwise nucleotide diversity (D_{xy}) for each gene as

$$D_{XY} = \frac{1}{n_x n_y} \sum_{i=1}^{n_x} \sum_{j=1}^{n_y} d_{ij}$$

using a custom script, where n_x is the number of *S. cerevisiae* strains, n_y is the number of *S. paradoxus* strains, and *d* is the number of sites with nucleotides differences at the same position for each pairwise sequence comparison. Sites with gaps or unknown nucleotides were ignored.

To test for enriched D_{xy} among thermotolerance genes in a given *S. cerevisiae* and *S paradoxus* population pair, we first tabulated D_{therm}, the median D_{xy} across the thermotolerance gene cohort. We next sampled 10,000 random cohorts of genes from the genome with the same number of essential and nonessential genes as in the thermotolerance cohort (Winzeler et al., 1999), and tabulated the D_{xy} in each D_{rand}. We used as an empirical *p*-value the proportion of random cohorts with $D_{rand} \geq D_{therm}$.

Multi-locus genotype and allele-sharing inference in *S. cerevisiae* populations

We calculated expected genotype homozygosity, G1; G12, expected genotype homozygosity with the frequencies of the two most frequent MLGs pooled into a single frequency; G2, expected genotype homozygosity omitting the most frequent MLG; and G2/G1 (Harris et al., 2018) as follows. We used unphased VCF genotypes for each of the five largest *S. cerevisiae* populations from 1011 Yeast Genomes (Peter et al., 2018) as input into SelectionHapStats (Harris et al., 2018) with the following parameters: -w (window size, SNPs) = 1200, and -j (jump size, SNPs) = 25. For each gene in the genome for which we had genotype calls, for a given population we tabulated a given statistic in each window whose center fell within the open reading frame, and we calculated the average across the windows.

In Table 1, to assess whether thermotolerance genes had a G1 distinct from those in the genome as a whole, we first calculated $G1_{therm}$, the median across our ten thermotolerance loci. We next sampled 10,000 random cohorts of genes from the genome with the same number of essential and nonessential genes as in the thermotolerance cohort (Winzeler et al., 1999), and for each we calculated the median G1, $G1_{rand}$. We then used as an empirical *p*-value the proportion of random cohorts with $G1_{rand} \geq G1_{therm}$, multiplying by 2 to render the test two-tailed. We followed the same strategy in Table 1 to calculate and assess enrichment of G2/G1 in

thermotolerance genes, except that we used a one-tailed resampling test. Because G2/G1 is usually interpreted in the context of G12 (Harris et al., 2018), we also used the above method to tabulate the latter in the five largest *S. cerevisiae* populations, which yielded enrichment for high values in each case, with empirical $p = 0.0631$ to 0.0009.

Separately, to check for effects of gene length, we devised a distinct analysis strategy in which random cohorts were resampled with the same length distribution as that of the true thermotolerance gene cohort; results for G1 in the Wine/European *S. cerevisiae* population mirrored those from essentiality-based resampling (data not shown).

Polymorphism in Wine/European *S. cerevisiae*

For the Wine/European *S. cerevisiae* population from (Peter et al., 2018), we used genotype data as a VCF as input into VCFtools (Danecek et al., 2011) with the command --site-pi. This output a polymorphism (π) value for each SNP. For Figure S1, we tabulated the average π across a 1200 SNP window centered at each SNP, with invariant sites contributing $\pi = 0$.

Custom scripts for sequence preparation and nucleotide diversity calculations are available at https://github.com/clairedubin/thermotolerance.

***ESP1* phylogenetic analysis**

We used the alignment of the open reading frame of *ESP1* from the type strains of *S. cerevisiae*, *S. paradoxus*, *S. mikatae*, *S. bayanus*, *S. uvarum*, and *S. kudriavzevii* from saccharomycessensustricto.org as input into the codeml module of PAML4.9 (Yang, 2007). The branch-site model (model=2, NSsites=2) was used, and two models, null and alternative, were fitted. In the null model, the dN/dS for the *S. cerevisiae* branch was fixed at 1.0 and all other branches were described by the same dN/dS ratio (ω). In the alternative model, the branch leading to *S. cerevisiae* was fitted with one ω, and all other branches were fitted with a separate ω. A test statistic, calculated by comparing the likelihood ratios of the alternative and null models, was used to calculate a *p*-value by comparing it to a chi-squared distribution with one degree of freedom, equal to the difference in the number of parameters in the two models. No codons exhibited a posterior probability of positive selection, on the branch leading to *S. cerevisiae*, higher than 0.9.

Analysis of *cis*-regulatory expression divergence between *S. cerevisiae* and *S. paradoxus*

In Table S4, we used measurements of high- and standard-temperature allele-specific expression in an *S. cerevisiae* x *S. uvarum* hybrid from (Schraiber et al., 2013) and in an *S. cerevisiae* x *S. paradoxus* hybrid from (Tirosh et al., 2009), as estimates of *cis*-regulatory variation between the respective species pairs at each thermotolerance gene.

Separately, we tested for directional, temperature-dependent *cis*-regulatory change across the thermotolerance gene cohort as follows. Using the data from (Li and Fay, 2017) for each gene in turn, given the allele-specific expression measurement $a_{T,Scer}$ from the *S. cerevisiae* allele at temperature T (37°C or 33°C), or $a_{T,Suv}$ calculated analogously for the *S. uvarum* allele, we tabulated the temperature-dependent allele-specific expression ratio ASE = $\log(a_{37,Scer}/a_{37,Suv}) - \log(a_{33,Scer}/a_{33,Suv})$. We took the median of this quantity across all thermotolerance genes ASE_{therm}. We next sampled 10,000 random cohorts of genes from the genome with the same number of essential and nonessential genes as in the thermotolerance cohort (Winzeler et al., 1999), and for each we calculated the median ASE, ASE_{rand}. We then used as an empirical *p*-value the proportion of random cohorts with $ASE_{rand} \geq ASE_{therm}$. Separately, we did the analogous calculation with the measurements from cultures at 35°C and 30°C from (Tirosh et al., 2009).

Interspecies swap strain construction at *ESP1* promoter and coding region

To swap the allele of the *ESP1* promoter from *S. paradoxus* Z1 into *S. cerevisiae* DBVPG1373, and likewise for the coding region, we designed allele-specific Cas9 guide RNAs for the *S. cerevisiae* background, generated donor DNA from *S. paradoxus*, transformed, and screened for successful transgenesis by Sanger sequencing as in (Weiss et al., 2018). Strains are listed in Table S5.

Large-format growth assay

For growth measurements in Figures 2 and S2, we assayed *S. paradoxus* Z1, *S. cerevisiae* DBVPG1373, the full *ESP1* swap in the *S. cerevisiae* background (harboring the promoter and

open reading frame from *S. paradoxus*) from (Weiss et al., 2018), and the *ESP1* promoter and coding swaps in the *S. cerevisiae* background (see above) as follows. Each strain was streaked from a -80°C freezer stock onto a yeast peptone dextrose (YPD) agar plate and incubated at room temperature for 3 days. For each biological replicate, a single colony was inoculated into 5 mL liquid YPD and grown for 24 hours at 28°C with shaking at 200 rpm to generate pre-cultures. Each pre-culture was back-diluted into YPD at an OD_{600} of 0.05 and grown for an additional 5.5-6 hours at 28°C, shaking at 200 rpm, until reaching logarithmic phase. Each pre-culture was again back-diluted into 10 mL YPD in 1-inch diameter glass tubes with a target OD_{600} of 0.05; the actual OD_{600} of each was measured, after which it was grown at either 28 or 39°C with shaking at 200rpm for 24 hours, and OD_{600} was measured again. The growth efficiency for each replicate was calculated as the difference between these final and initial OD_{600} values. The pipeline from inoculation off of solid plates through preculture, two back-dilutions, and growth at 28 or 39°C we refer to as a day's growth experiment. For each day's experiments, we calculated the average efficiency $\langle e_{Scer} \rangle$ across the replicates of wild-type *S. cerevisiae*, and we used this quantity to normalize the efficiency e_s measured for each replicate assayed on that day of a strain of interest *s*. Thus, the final measurement used for analysis for each replicate on a given day was $e_s/\langle e_{Scer} \rangle$. We carried out a total of 2-3 days' worth of replicate growth experiments. We used the complete cohort of measurements of $e_s/\langle e_{Scer} \rangle$ from all days as input into a one-sample, one-tailed Wilcoxon test to evaluate whether $e_s/\langle e_{Scer} \rangle$ was less than 1 (*i.e.* that the strain grew worse at 39°C than wild-type *S. cerevisiae*).

Temperature dose-response growth assay

To evaluate temperature dose-responses in Figure 4, we assayed *S. paradoxus* Z1, *S. cerevisiae* DBVPG1373, and the full *ESP1* swap in the *S. cerevisiae* background (harboring the promoter and open reading frame from *S. paradoxus*) from (Weiss et al., 2018) as follows. Each strain was streaked from a -80°C freezer stock onto a YPD agar plate and incubated at room temperature for 3 days. For each biological replicate, a single colony was inoculated into 5 mL liquid YPD and grown for 48 hours at 28°C with shaking at 200 rpm to create a stationary phase pre-culture. From pre-culture we made eight back-dilution experimental cultures in a standard PCR strip tube, each in 200 µL YPD, and we incubated these in a thermocycler using a gradient protocol from 37.0 to 40.8°C. After 24 hours, 150 µL from each culture was removed and OD_{600} was measured. The pipeline from inoculation off of solid plates through pre-culture, back-dilution, and growth we refer to as a day's growth experiment for the dose-response of a strain.

For each day's experiments, at a given temperature we calculated the average efficiency $\langle e_{Scer,37} \rangle$ across the replicates of wild-type *S. cerevisiae* at 37°C, and used it to normalize the efficiency $e_{s,T}$ measured for each replicate assayed on that day of a strain of interest *s* at temperature T. Thus, the final measurement used for analysis for each replicate and temperature on a given day was $e_{s,T}/\langle e_{Scer,37} \rangle$. We carried out two days' worth of replicate growth experiments, and used the complete cohort of measurements of $e_{s,T}/\langle e_{Scer,37} \rangle$ from all days and all temperatures as input into a two-factor type 2 ANOVA test for a temperature-by-strain effect comparing *s* with *S. cerevisiae*.

Microscopy

Microscopy was performed as described in (Weiss et al., 2018). Images were scored, blinded, for the size of dyads, omitting all clumps of >2 cells. Two replicates per strain and condition were imaged, and ten to sixteen images per replicate were scored. Significance was evaluated using a two-factor ANOVA test to evaluate strain by temperature effects.

ACKNOWLEDGEMENTS

The authors thank Julie Chuong for verifying and maintaining transgenic strains, David Savage for his generosity with lab facilities and resources, Josh Schraiber for invaluable discussions, and Jeremy Roop for critical reading of the manuscript. This work was supported by NSF GRFP DGE 1752814 to M.A. and NIH R01 GM120430 to R.B.B.

BIBLIOGRAPHY

Anderson, D.P., Whitney, D.S., Hanson-Smith, V., Woznica, A., Campodonico-Burnett, W., Volkman, B.F., King, N., Thornton, J.W., and Prehoda, K.E. (2016). Evolution of an ancient protein function involved in organized multicellularity in animals. ELife *5*, e10147.

Anderson, D.W., McKeown, A.N., and Thornton, J.W. (2015). Intermolecular epistasis shaped the function and evolution of an ancient transcription factor and its DNA binding sites. ELife *4*, e07864.

Asgari, S., Luo, Y., Akbari, A., Belbin, G.M., Li, X., Harris, D.N., Selig, M., Bartell, E., Calderon, R., Slowikowski, K., et al. (2020). A positively selected FBN1 missense variant reduces height in Peruvian individuals. Nature *582*, 234–239.

Baldwin, M.W., Toda, Y., Nakagita, T., O'Connell, M.J., Klasing, K.C., Misaka, T., Edwards, S.V., and Liberles, S.D. (2014). Sensory biology. Evolution of sweet taste perception in hummingbirds by transformation of the ancestral umami receptor. Science (New York, N.Y.) *345*, 929–933.

Barroso-Batista, J., Sousa, A., Lourenço, M., Bergman, M.-L., Sobral, D., Demengeot, J., Xavier, K.B., and Gordo, I. (2014). The first steps of adaptation of Escherichia coli to the gut are dominated by soft sweeps. PLoS Genetics *10*, e1004182.

Bergström, A., Simpson, J.T., Salinas, F., Barré, B., Parts, L., Zia, A., Nguyen Ba, A.N., Moses, A.M., Louis, E.J., Mustonen, V., et al. (2014). A high-definition view of functional genetic variation from natural yeast genomes. Mol. Biol. Evol. *31*, 872–888.

Berry, A.J., Ajioka, J.W., and Kreitman, M. (1991). Lack of polymorphism on the Drosophila fourth chromosome resulting from selection. Genetics *129*, 1111–1117.

Blount, Z.D., Barrick, J.E., Davidson, C.J., and Lenski, R.E. (2012). Genomic analysis of a key innovation in an experimental Escherichia coli population. Nature *489*, 513–518.

Bridgham, J.T., Ortlund, E.A., and Thornton, J.W. (2009). An epistatic ratchet constrains the direction of glucocorticoid receptor evolution. Nature *461*, 515–519.

Bullard, J.H., Mostovoy, Y., Dudoit, S., and Brem, R.B. (2010). Polygenic and directional regulatory evolution across pathways in Saccharomyces. Proc. Natl. Acad. Sci. U.S.A. *107*, 5058–5063.

Castro, J.P., Yancoskie, M.N., Marchini, M., Belohlavy, S., Hiramatsu, L., Kučka, M., Beluch, W.H., Naumann, R., Skuplik, I., Cobb, J., et al. (2019). An integrative genomic analysis of the Longshanks selection experiment for longer limbs in mice. ELife *8*, e42014.

Chan, Y.F., Marks, M.E., Jones, F.C., Villarreal, G., Shapiro, M.D., Brady, S.D., Southwick, A.M., Absher, D.M., Grimwood, J., Schmutz, J., et al. (2010). Adaptive evolution of pelvic reduction in sticklebacks by recurrent deletion of a Pitx1 enhancer. Science (New York, N.Y.) *327*, 302–305.

Cleves, P.A., Ellis, N.A., Jimenez, M.T., Nunez, S.M., Schluter, D., Kingsley, D.M., and Miller, C.T. (2014). Evolved tooth gain in sticklebacks is associated with a cis-regulatory allele of Bmp6. PNAS *111*, 13912–13917.

Danecek, P., Auton, A., Abecasis, G., Albers, C.A., Banks, E., DePristo, M.A., Handsaker, R.E., Lunter, G., Marth, G.T., Sherry, S.T., et al. (2011). The variant call format and VCFtools. Bioinformatics *27*, 2156–2158.

Durand, É., Gagnon-Arsenault, I., Hallin, J., Hatin, I., Dubé, A.K., Nielly-Thibault, L., Namy, O., and Landry, C.R. (2019). Turnover of ribosome-associated transcripts from de novo ORFs produces gene-like characteristics available for de novo gene emergence in wild yeast populations. Genome Res. *29*, 932–943.

Edgar, R.C. (2004). MUSCLE: multiple sequence alignment with high accuracy and high throughput. Nucleic Acids Res. *32*, 1792–1797.

Field, Y., Boyle, E.A., Telis, N., Gao, Z., Gaulton, K.J., Golan, D., Yengo, L., Rocheleau, G., Froguel, P., McCarthy, M.I., et al. (2016). Detection of human adaptation during the past 2000 years. Science *354*, 760–764.

Finnigan, G.C., Hanson-Smith, V., Stevens, T.H., and Thornton, J.W. (2012). Evolution of increased complexity in a molecular machine. Nature *481*, 360–364.

Garud, N.R., Messer, P.W., Buzbas, E.O., and Petrov, D.A. (2015). Recent Selective Sweeps in North American Drosophila melanogaster Show Signatures of Soft Sweeps. PLoS Genet *11*, e1005004.

Gonçalves, P., Valério, E., Correia, C., de Almeida, J.M.G.C.F., and Sampaio, J.P. (2011). Evidence for Divergent Evolution of Growth Temperature Preference in Sympatric Saccharomyces Species. PLoS One *6*.

Good, B.H., McDonald, M.J., Barrick, J.E., Lenski, R.E., and Desai, M.M. (2017). The dynamics of molecular evolution over 60,000 generations. Nature *551*, 45–50.

Harris, A.M., Garud, N.R., and DeGiorgio, M. (2018). Detection and Classification of Hard and Soft Sweeps from Unphased Genotypes by Multilocus Genotype Identity. Genetics *210*, 1429–1452.

Hoekstra, H.E., and Coyne, J.A. (2007). The locus of evolution: evo devo and the genetics of adaptation. Evolution; International Journal of Organic Evolution *61*, 995–1016.

Hoekstra, H.E., and Nachman, M.W. (2003). Different genes underlie adaptive melanism in different populations of rock pocket mice. Molecular Ecology *12*, 1185–1194.

Leuenberger, P., Ganscha, S., Kahraman, A., Cappelletti, V., Boersema, P.J., von Mering, C., Claassen, M., and Picotti, P. (2017). Cell-wide analysis of protein thermal unfolding reveals determinants of thermostability. Science (New York, N.Y.) *355*.

Li, X.C., and Fay, J.C. (2017). Cis-Regulatory Divergence in Gene Expression between Two Thermally Divergent Yeast Species. Genome Biol Evol *9*, 1120–1129.

Linnen, C.R., Poh, Y.-P., Peterson, B.K., Barrett, R.D.H., Larson, J.G., Jensen, J.D., and Hoekstra, H.E. (2013). Adaptive Evolution of Multiple Traits Through Multiple Mutations at a Single Gene. Science *339*, 1312–1316.

Liu, Q., Onal, P., Datta, R.R., Rogers, J.M., Schmidt-Ott, U., Bulyk, M.L., Small, S., and Thornton, J.W. (2018). Ancient mechanisms for the evolution of the bicoid homeodomain's function in fly development. ELife *7*.

Lynch, M. (2010). Scaling expectations for the time to establishment of complex adaptations. Proceedings of the National Academy of Sciences of the United States of America *107*, 16577–16582.

Massey, J., and Wittkopp, P.J. (2016). The genetic basis of pigmentation differences within and between Drosophila species. Curr Top Dev Biol *119*, 27–61.

Messer, P.W., and Petrov, D.A. (2013). Population genomics of rapid adaptation by soft selective sweeps. Trends Ecol. Evol. (Amst.) *28*, 659–669.

Neher, R.A., Shraiman, B.I., and Fisher, D.S. (2010). Rate of adaptation in large sexual populations. Genetics *184*, 467–481.

Nei, M. (1987). Molecular Evolutionary Genetics (Columbia University Press).

Peter, J., De Chiara, M., Friedrich, A., Yue, J.-X., Pflieger, D., Bergström, A., Sigwalt, A., Barre, B., Freel, K., Llored, A., et al. (2018). Genome evolution across 1,011 Saccharomyces cerevisiae isolates. Nature *556*, 339–344.

Pillai, A.S., Chandler, S.A., Liu, Y., Signore, A.V., Cortez-Romero, C.R., Benesch, J.L.P., Laganowsky, A., Storz, J.F., Hochberg, G.K.A., and Thornton, J.W. (2020). Origin of complexity in haemoglobin evolution. Nature *581*, 480–485.

Robinson, H.A., Pinharanda, A., and Bensasson, D. (2016). Summer temperature can predict the distribution of wild yeast populations. Ecology and Evolution *6*, 1236–1250.

Rosenblum, E.B., Römpler, H., Schöneberg, T., and Hoekstra, H.E. (2010). Molecular and functional basis of phenotypic convergence in white lizards at White Sands. Proceedings of the National Academy of Sciences of the United States of America *107*, 2113–2117.

Sackton, T.B., Grayson, P., Cloutier, A., Hu, Z., Liu, J.S., Wheeler, N.E., Gardner, P.P., Clarke, J.A., Baker, A.J., Clamp, M., et al. (2019). Convergent regulatory evolution and loss of flight in paleognathous birds. Science (New York, N.Y.) *364*, 74–78.

Salvadó, Z., Arroyo-López, F.N., Guillamón, J.M., Salazar, G., Querol, A., and Barrio, E. (2011). Temperature adaptation markedly determines evolution within the genus Saccharomyces. Applied and Environmental Microbiology *77*, 2292–2302.

Sas-Chen, A., Thomas, J.M., Matzov, D., Taoka, M., Nance, K.D., Nir, R., Bryson, K.M., Shachar, R., Liman, G.L.S., Burkhart, B.W., et al. (2020). Dynamic RNA acetylation revealed by quantitative cross-evolutionary mapping. Nature *583*, 638–643.

Schraiber, J.G., Mostovoy, Y., Hsu, T.Y., and Brem, R.B. (2013). Inferring evolutionary histories of pathway regulation from transcriptional profiling data. PLoS Comput. Biol. *9*, e1003255.

Smith, J.M., and Haigh, J. (1974). The hitch-hiking effect of a favourable gene. Genetical Research *23*, 23–35.

Steinmetz, L.M., Sinha, H., Richards, D.R., Spiegelman, J.I., Oefner, P.J., McCusker, J.H., and Davis, R.W. (2002). Dissecting the architecture of a quantitative trait locus in yeast. Nature *416*, 326–330.

Stern, D.L. (2014). Identification of loci that cause phenotypic variation in diverse species with the reciprocal hemizygosity test. Trends in Genetics *30*, 547–554.

Sulak, M., Fong, L., Mika, K., Chigurupati, S., Yon, L., Mongan, N.P., Emes, R.D., and Lynch, V.J. (2016). TP53 copy number expansion is associated with the evolution of increased body size and an enhanced DNA damage response in elephants. ELife *5*.

Sweeney, J.Y., Kuehne, H.A., and Sniegowski, P.D. (2004). Sympatric natural Saccharomyces cerevisiae and S. paradoxus populations have different thermal growth profiles. FEMS Yeast Research *4*, 521–525.

Tenaillon, O., Barrick, J.E., Ribeck, N., Deatherage, D.E., Blanchard, J.L., Dasgupta, A., Wu, G.C., Wielgoss, S., Cruveiller, S., Médigue, C., et al. (2016). Tempo and mode of genome evolution in a 50,000-generation experiment. Nature *536*, 165–170.

Tian, X., Firsanov, D., Zhang, Z., Cheng, Y., Luo, L., Tombline, G., Tan, R., Simon, M., Henderson, S., Steffan, J., et al. (2019). SIRT6 Is Responsible for More Efficient DNA Double-Strand Break Repair in Long-Lived Species. Cell *177*, 622-638.e22.

Tirosh, I., Reikhav, S., Levy, A.A., and Barkai, N. (2009). A Yeast Hybrid Provides Insight into the Evolution of Gene Expression Regulation. Science *324*, 659–662.

Toprak, E., Veres, A., Michel, J.-B., Chait, R., Hartl, D.L., and Kishony, R. (2011). Evolutionary paths to antibiotic resistance under dynamically sustained drug selection. Nature Genetics *44*, 101–105.

Weigand, H., and Leese, F. (2018). Detecting signatures of positive selection in non-model species using genomic data. Zool J Linn Soc *184*, 528–583.

Weiss, C.V., and Brem, R.B. (2019). Dissecting Trait Variation across Species Barriers. Trends in Ecology & Evolution *34*, 1131–1136.

Weiss, C.V., Roop, J.I., Hackley, R.K., Chuong, J.N., Grigoriev, I.V., Arkin, A.P., Skerker, J.M., and Brem, R.B. (2018). Genetic dissection of interspecific differences in yeast thermotolerance. Nat Genet *50*, 1501–1504.

Will, J.L., Kim, H.S., Clarke, J., Painter, J.C., Fay, J.C., and Gasch, A.P. (2010). Incipient balancing selection through adaptive loss of aquaporins in natural Saccharomyces cerevisiae populations. PLoS Genet. *6*, e1000893.

Winzeler, E.A., Shoemaker, D.D., Astromoff, A., Liang, H., Anderson, K., Andre, B., Bangham, R., Benito, R., Boeke, J.D., Bussey, H., et al. (1999). Functional characterization of the S. cerevisiae genome by gene deletion and parallel analysis. Science *285*, 901–906.

Wray, G.A. (2007). The evolutionary significance of cis-regulatory mutations. Nature Reviews. Genetics *8*, 206–216.

Xie, K.T., Wang, G., Thompson, A.C., Wucherpfennig, J.I., Reimchen, T.E., MacColl, A.D.C., Schluter, D., Bell, M.A., Vasquez, K.M., and Kingsley, D.M. (2019). DNA fragility in the parallel evolution of pelvic reduction in stickleback fish. Science *363*, 81–84.

Yang, Z. (2007). PAML 4: phylogenetic analysis by maximum likelihood. Mol. Biol. Evol. *24*, 1586–1591.

FIGURE LEGENDS

Figure 1. A peak of high allele frequency in *S. cerevisiae* populations at the 5' end of *ESP1*. Each panel shows results of analysis of allele frequency at the thermotolerance gene *ESP1* in a population of *S. cerevisiae* from (Peter et al., 2018). In each panel, the *y*-axis reports genotype homozygosity, G1, in a 1200-SNP window around the position shown on the *x*. The *ESP1* open reading frame is demarcated with a dark black arrow (direction of transcription is right to left). **A**, Wine/European population. **B**, Mosaic Region 3 population. **C**, Brazilian Bioethanol population.

Figure 2. The *S. cerevisiae ESP1* coding region, but not the promoter, is required for thermotolerance. Each column represents results from biomass accumulation assays of a wild-type or transgenic yeast strain cultured at high temperature. The *y*-axis reports the optical density of a culture of the indicated strain after 24h at 39°C, normalized to the analogous quantity from wild-type *S. cerevisiae* (dashed line). Each point reports results from one biological replicate, and each bar height reports the average across replicates (n = 6-12). The first two columns report results from wild-type (WT) strains of *S. paradoxus* Z1 (Sp) and *S. cerevisiae* DBVPG17373 (Sc). The last three columns report strains with the indicated region of *ESP1* from *S. paradoxus* swapped into *S. cerevisiae* at the endogenous location; *ESP1* full swap denotes transgenesis of both the promoter and the coding region. *, Wilcoxon test $p < 0.02$ in a comparison against wild-type *S. cerevisiae*. Culture data at 28°C are given in Figure S2.

Figure 3. Growth function of *S. paradoxus ESP1* declines sharply with temperature. Each trace reports results from biomass accumulation assays of a wild-type or transgenic yeast strain across temperatures. Strain labels are as in Figure 2. The *y*-axis reports the optical density of a culture of the indicated strain after 24h at the temperature on the *x*, normalized to the optical density of that day's wild-type *S. cerevisiae* at 37°C. *, $p < 10^{-12}$ for the strain by temperature interaction term of a two-factor ANOVA, in a comparison between the indicated strain and wild-type *S. cerevisiae*.

Figure 4. The *S. paradoxus* allele of *ESP1* compromises cell division at high temperature. **A**, Each panel reports a representative image of a wild-type or transgenic yeast strain after incubation for 24h at the indicated temperature. Strain labels are as in Figure 2. **B**, Each bar reports quantification of replicated imaging data of the indicated strain cultured at the indicated temperature, as in **A**. For each bar, the *y*-axis shows the fraction of dyads in the indicated size category. *, $p < 0.015$ for the strain by temperature interaction term of a two-factor ANOVA, in a comparison between the indicated strain and wild-type *S. cerevisiae*.

TABLES

		G1[a]			G2/G1[b]		
Population	**# Isolates**	**Thermotolerance genes**	**Genome**	***p***	**Thermotolerance genes**	**Genome**	***p***
Wine/European	362	0.048	0.026	0.0101*	0.362	0.602	0.0484*
Mosaic Region 3	113	0.022	0.019	0.0492*	0.803	0.819	0.669
Mixed Origin	72	0.077	0.061	0.0677	0.688	0.715	0.290
Sake	47	0.278	0.257	0.0608	0.158	0.130	0.609
Brazilian Bioethanol	35	0.133	0.109	0.0284*	0.263	0.363	0.0456*

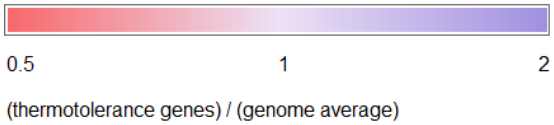

Table 1. Thermotolerance loci are enriched for allele-sharing within *S. cerevisiae* populations.

[a]For the *S. cerevisiae* population indicated in a given row, the columns report the median value of the allele-sharing statistic genotype homozygosity, G1, in thermotolerance genes and random sets of genes from the genome, respectively, and empirical significance from a resampling test. [b]Data are as in *a* except that the metric analyzed was homozygosity calculated from all genotypes except the most common one, G2, normalized by G1. *, $p < 0.05$. Colors report the ratio of the median of the respective metric across thermotolerance loci to that across the genome.

FIGURE 1

A.

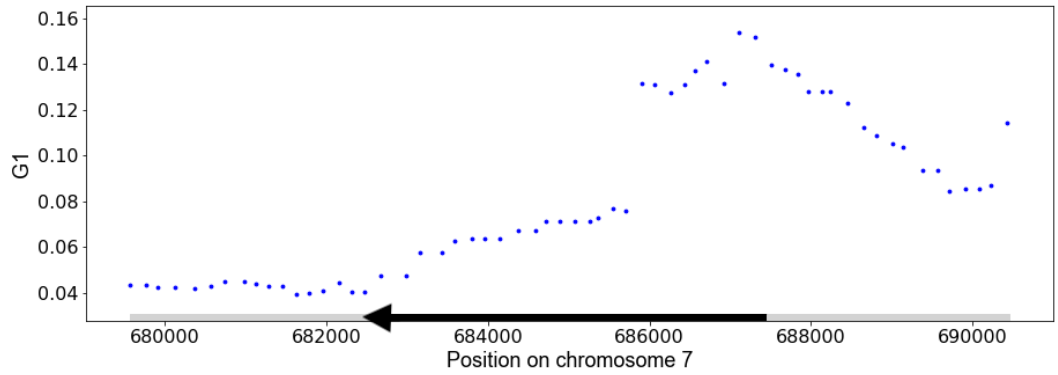

B.

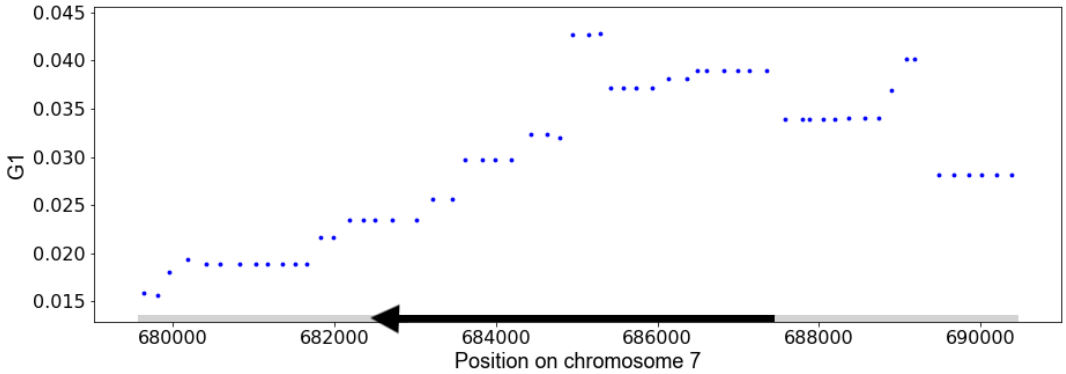

C.

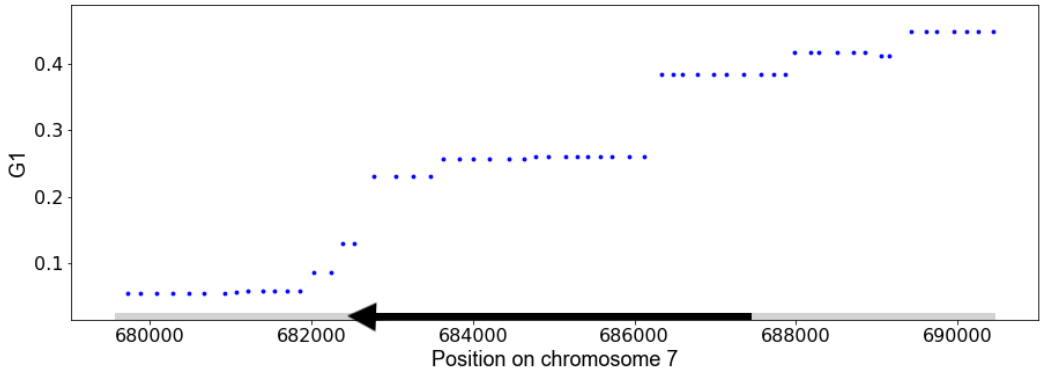

FIGURE 2

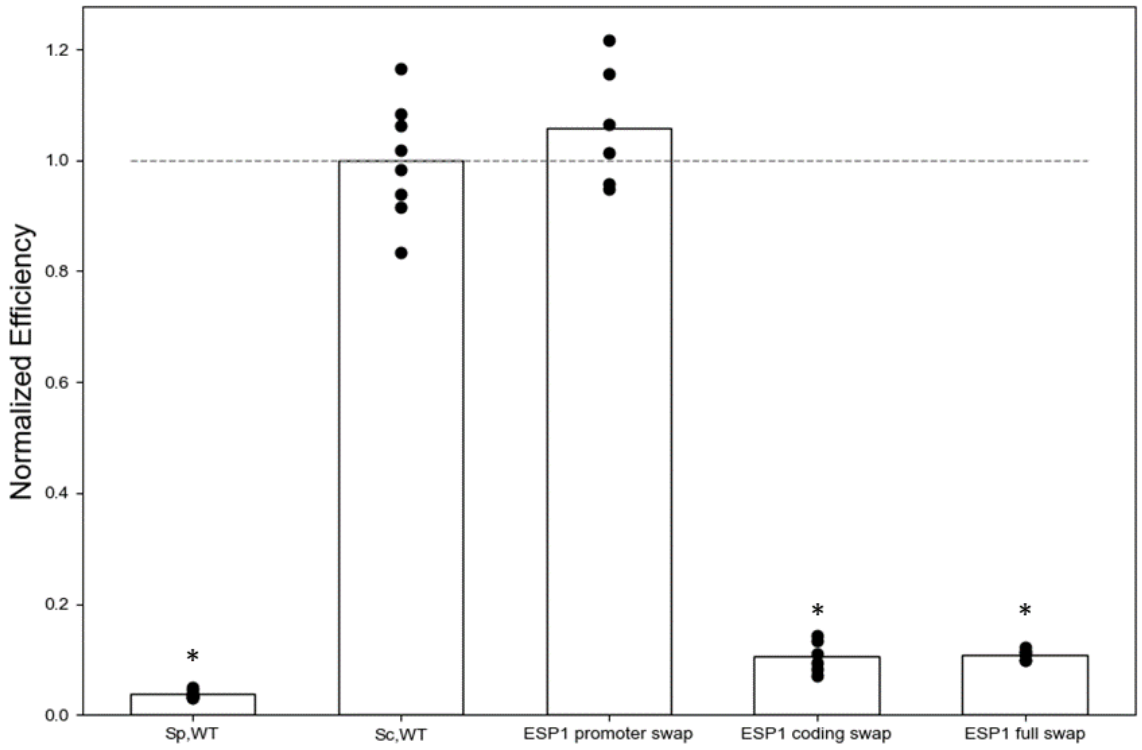

FIGURE 3

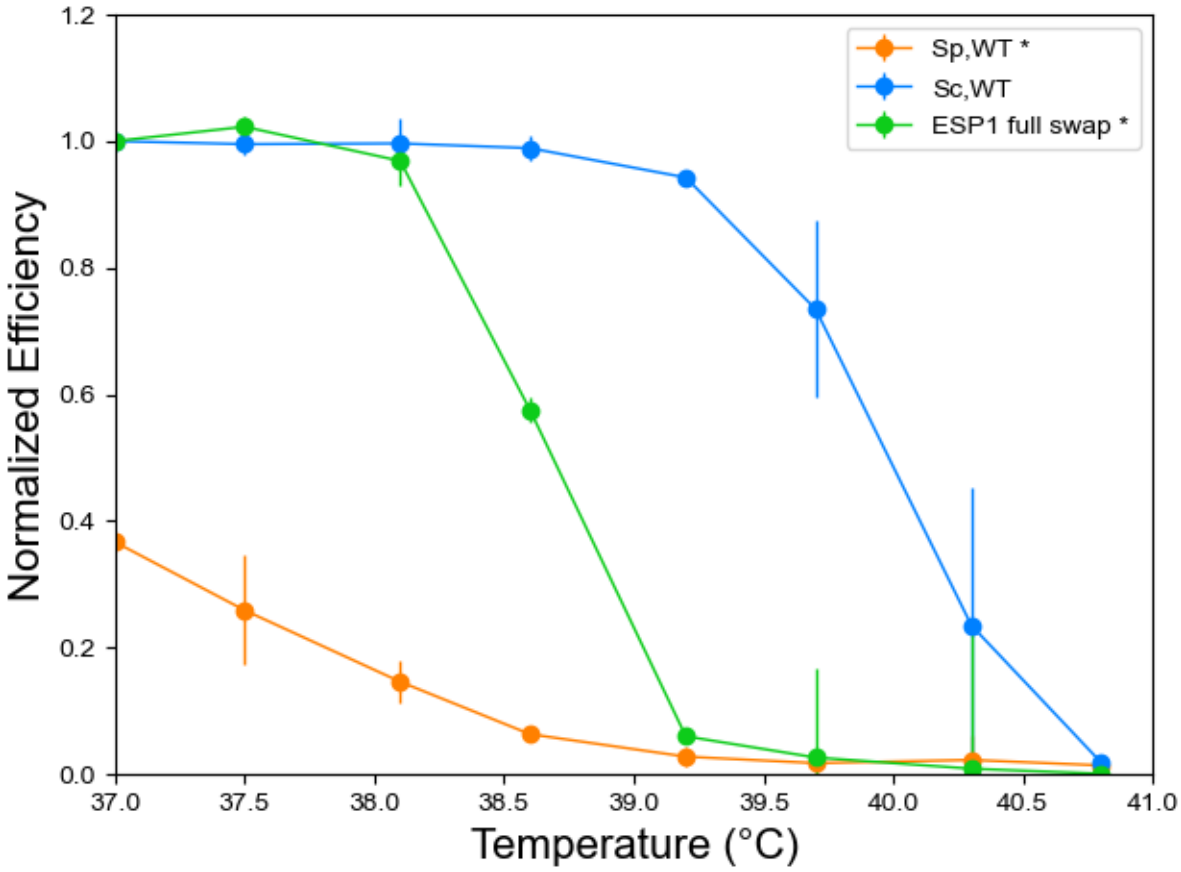

FIGURE 4

A.

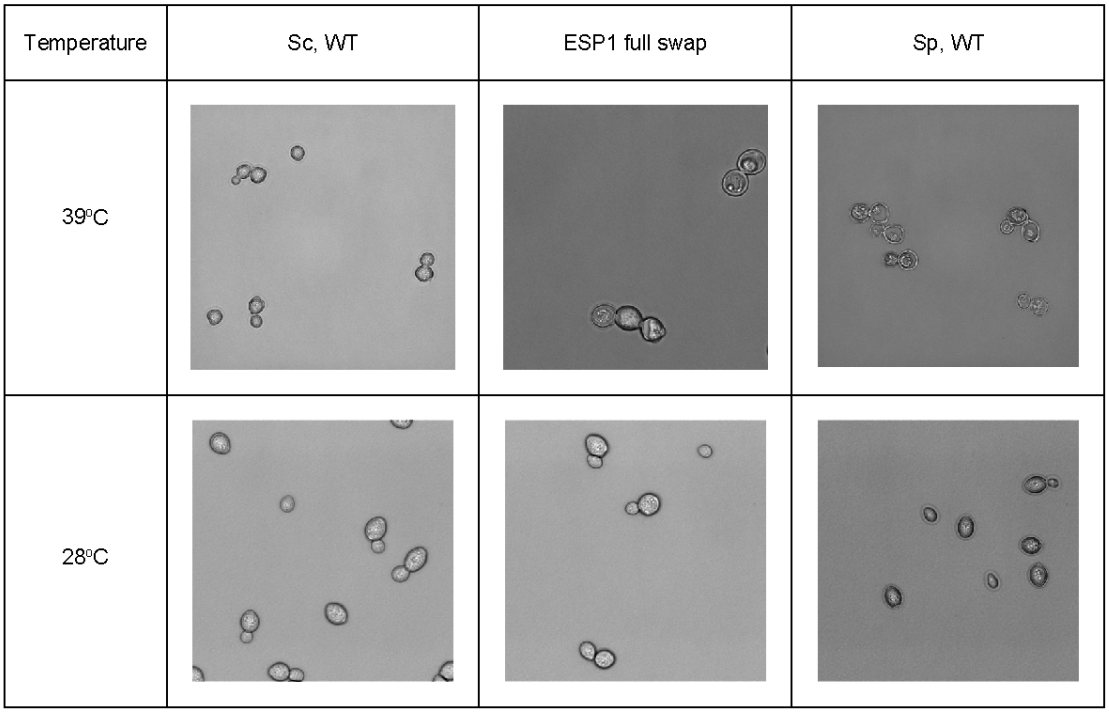

B.